Materials and Methods

All reagents were commercially available and used as supplied without further purification. Compounds **1**[S1], **TA**[S2] and **TI**[S3] were synthesized according to previous literature reports. Activated crystalline **TI** was recrystallized from a mixture of chloroform and ethanol and dried under vacuum at 120 °C for one day. Activated crystalline **TA** was recrystallized from ethanol and dried under vacuum at 120 °C for one day. Activated crystalline **MTA** was recrystallized from a mixture of chloroform and ethanol and dried under vacuum at 120 °C for one day.

NMR spectra were recorded with a Bruker Avance DMX 400 and 500 spectrophotometers with TMS as the internal reference.

The crystal data was collected using a Bruker X8 Prospector APEX2 CCD (Cu *K*α radiation, λ = 1.54178 Å) or a D8 Venture with Photon II CPAD diffractometer (Mo *K*α radiation, λ = 0.71073 Å).

Gas chromatography (GC) measurements were carried out using J&W (122-1364) instrument configured with a FID detector and a DB-624 column (60 m × 0.25 mm × 1.4 μm). The following GC method was used: the oven was programmed from 50 °C, ramped at 15 °C min^{-1} increments to 200 °C with 15 min hold; the total run time was 25 min; injection temperature 250 °C; detector temperature 300 °C with hydrogen, air, and make-up flow-rates of 35, 350, and 30 mL min^{-1}, respectively; helium (carrier gas) flow-rate 3.0 mL min^{-1}. The powder samples (20 mg) were dissolved in 1 mL dichloromethane and injected in the split mode (4:1).

Thermogravimetric analysis was carried out using an automatic sample loading TA Instruments Q50 analyzer. The samples were heated starting at room temperature to 800 °C using N_2 as the protective gas.

Low-pressure gas adsorption measurements were performed on a Micrometritics Accelerated Surface Area and Porosimetry System (ASAP) 2020 surface area analyzer. Samples were degassed under dynamic vacuum for 12 h at 60 °C prior to each measurement. N_2 isotherms were measured using a liquid nitrogen bath (77 K).

Synthesis of MTA

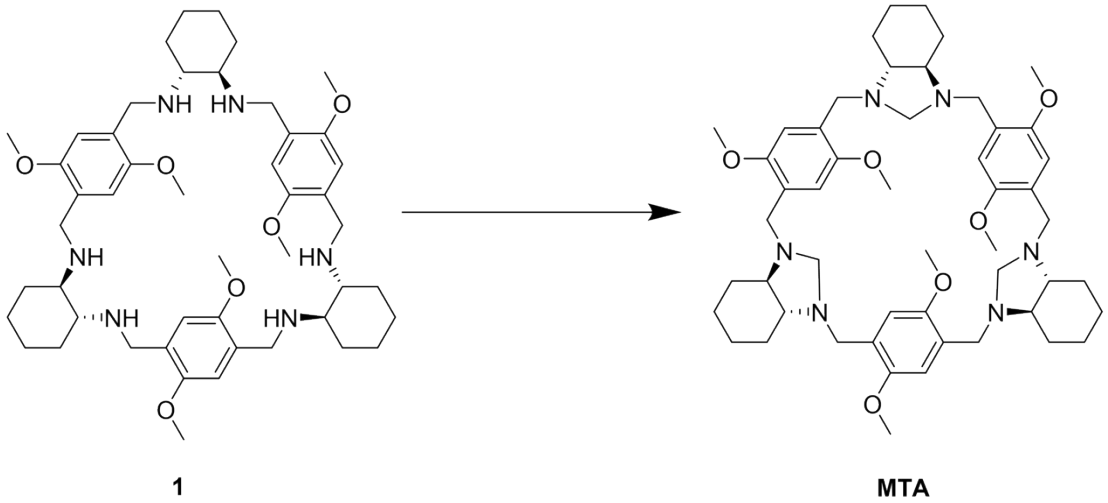

Figure S1. The synthetic route of **MTA**

A solution of trianglamine **1** (414 mg, 0.5 mmol) and paraformaldehyde (180 mg, 6 mmol) in a mixture of chloroform (10 mL) and ethanol (10 mL) was heated at reflux for 12 h. After cooling, the white product was filtered off and washed with ethanol. Yield: 350 mg (81%).

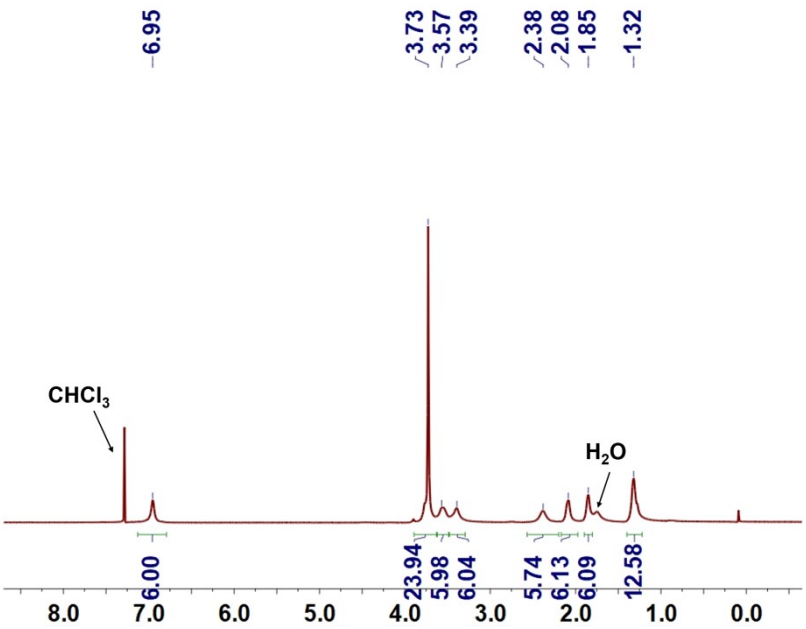

Figure S2. ^{1}H NMR spectrum (400 MHz, $CDCl_3$, 293 K) of **MTA**. δ (ppm): 6.95 (s, 6H), 3.73 (s, 24H), 3.57 (s, 6H), 3.39 (s, 6H), 2.38C (S, 6H), 2.08 (s, 6H), 1.85 (s, 6H), 1.32 (s, 12H).

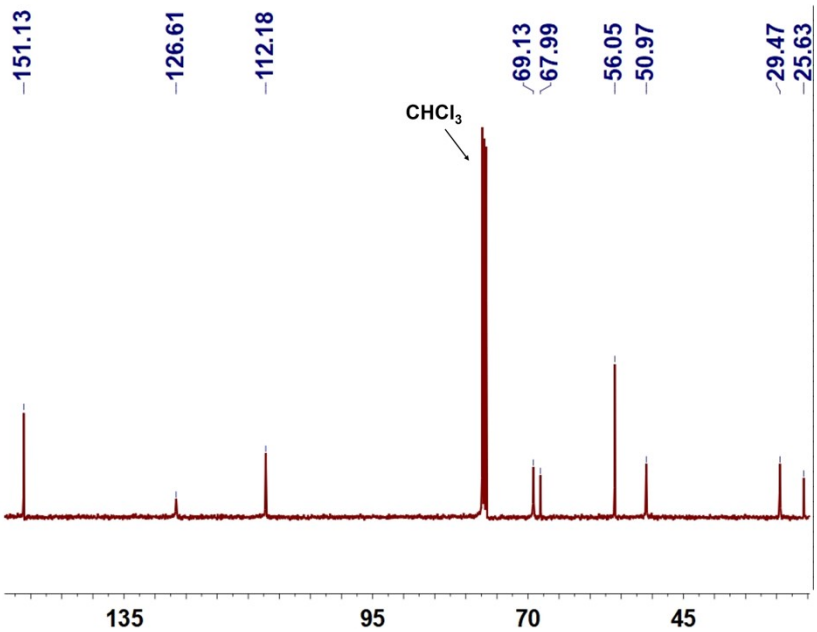

Figure S3. ^{13}C NMR spectrum (100 MHz, $CDCl_3$, 293 K) of **MTA**. δ (ppm): 151.13, 126.61, 112.18, 69.13, 67.99, 56.05, 50.97, 29.47, 25.63.

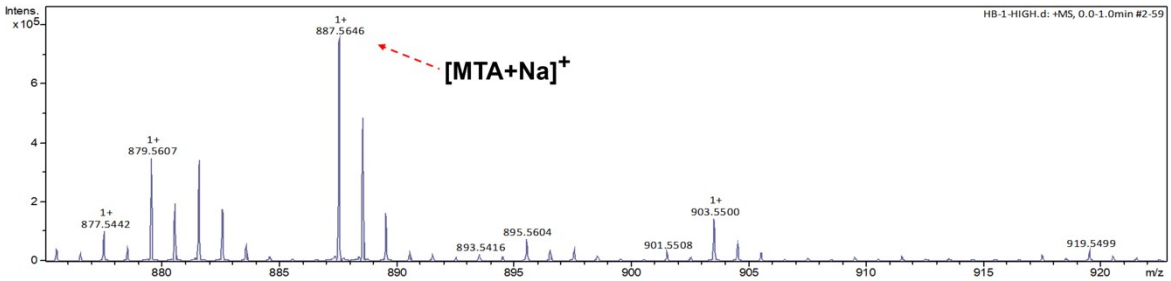

Figure S4. ESI-Mass spectrum of **MTA**.

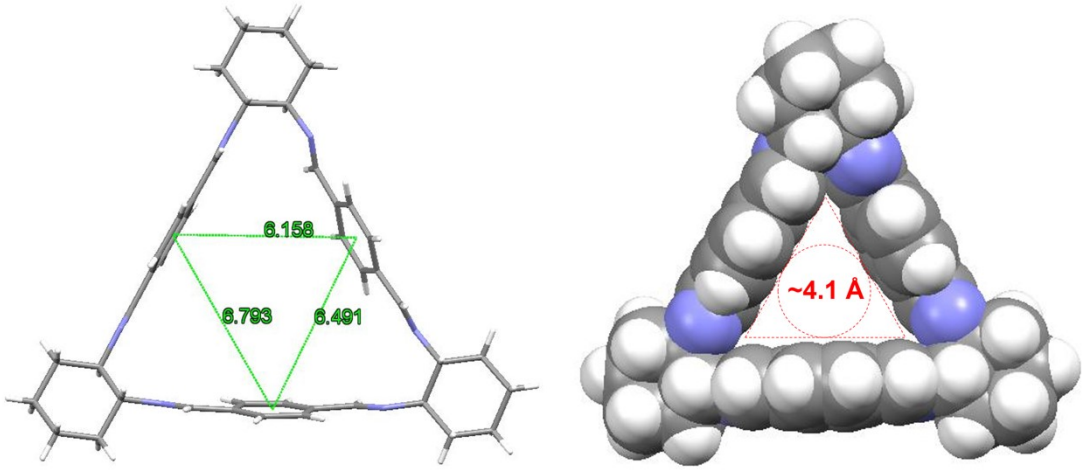

Figure S5. The estimated cavity size of **TI** (CCDC number: 143138).

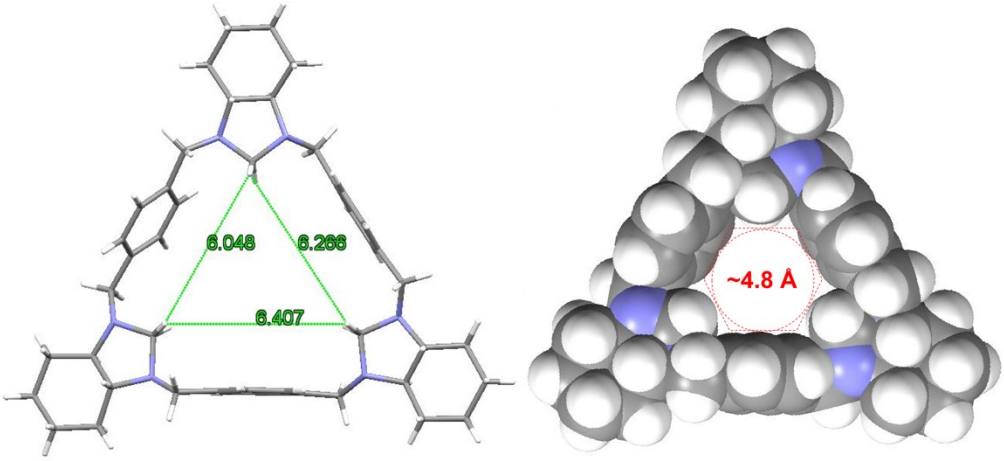

Figure S6. The estimated cavity size of **TA** (CCDC number: 2056802).

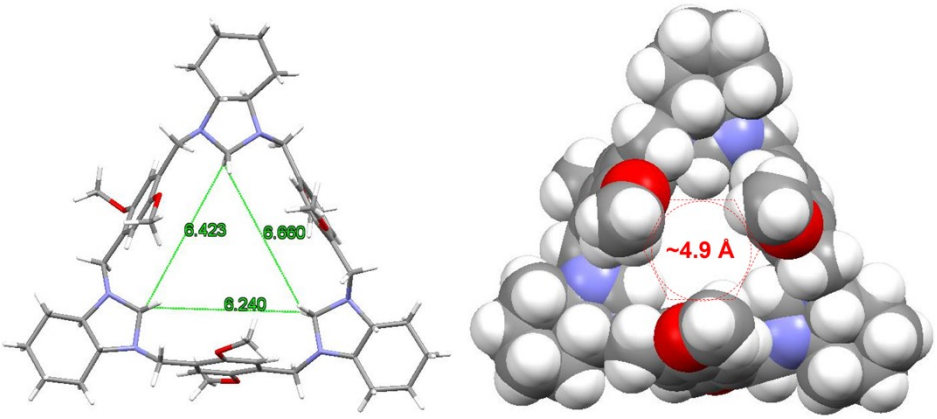

Figure S7. The estimated cavity size of **MTA** (CCDC number: 2056800).

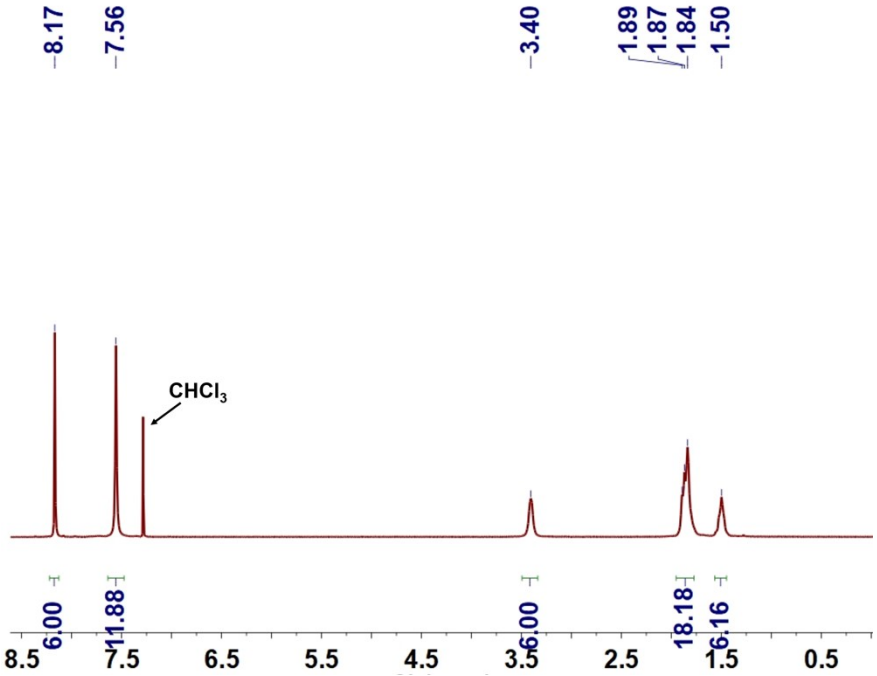

Figure S8. ^{1}H NMR spectrum (400 MHz, $CDCl_3$, 293 K) of activated **TI**.

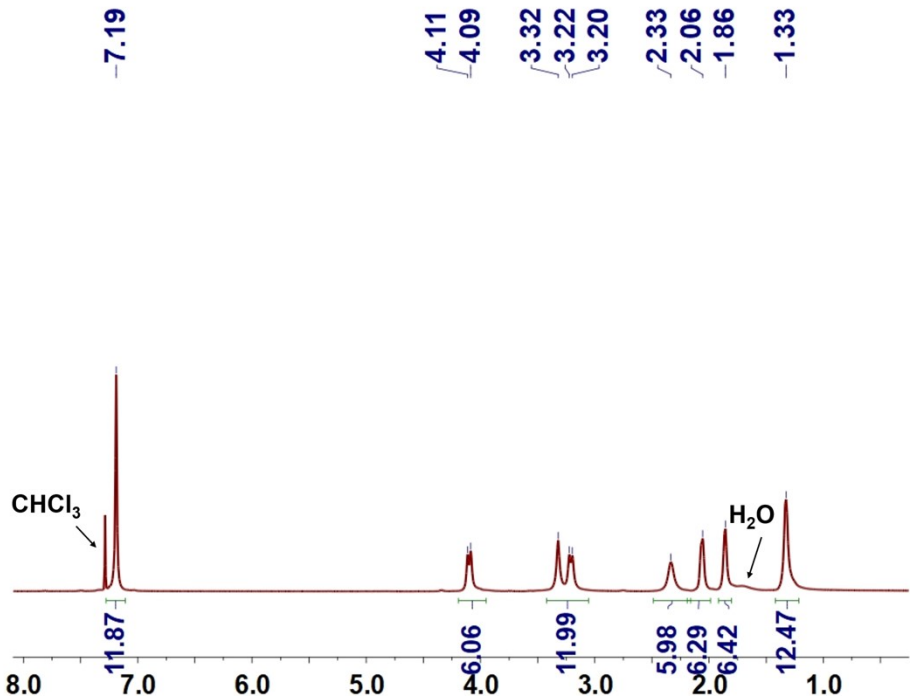

Figure S9. ^{1}H NMR spectrum (400 MHz, $CDCl_3$, 293 K) of activated **TA**. The H_2O peak is from $CDCl_3$.

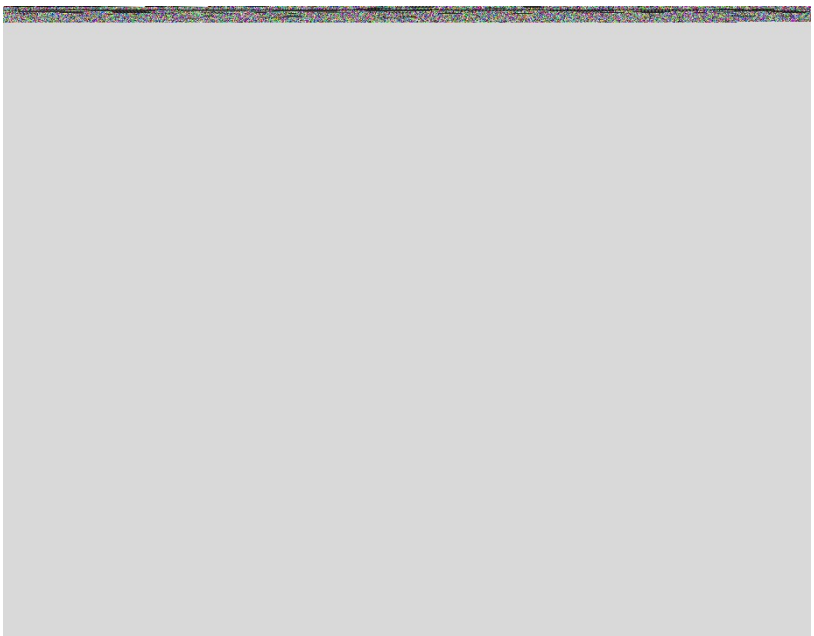

Figure S10. ^{1}H NMR spectrum (400 MHz, $CDCl_3$, 293 K) of activated **MTA**. The H_2O peak is from $CDCl_3$.

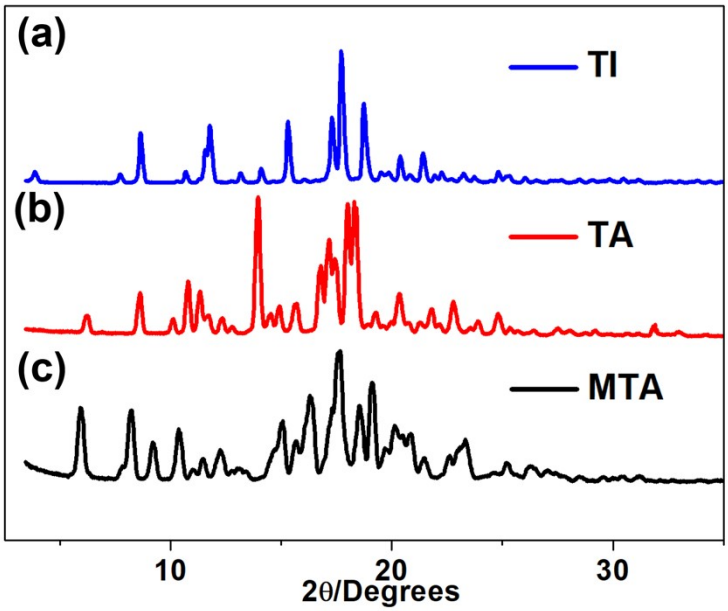

Figure S11. Powder X-ray diffraction patterns: (a) activated **TI** crystals; (b) activated **TA** crystals and (c) activated **MTA** crystals.

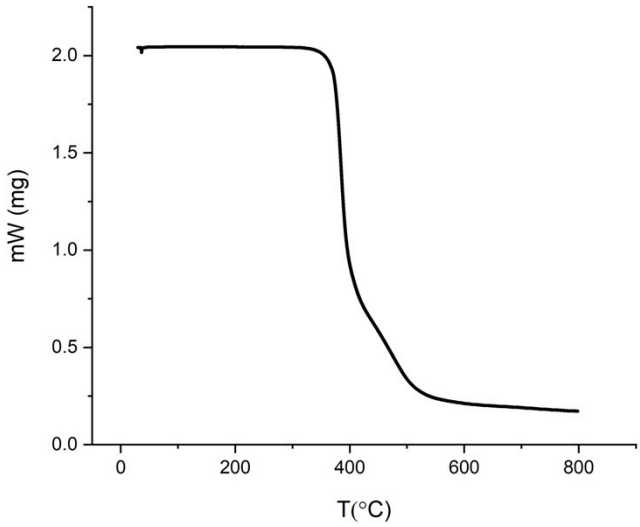

Figure S12. Thermogravimetric analysis of activated **TI**.

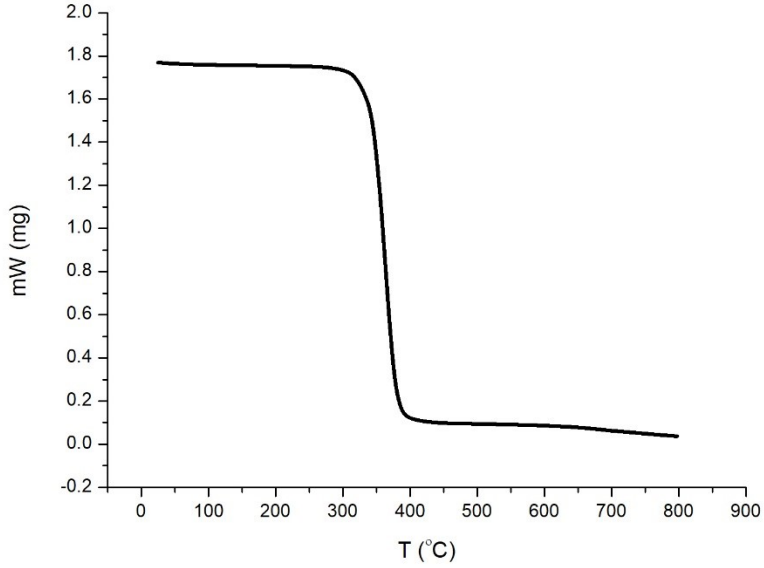

Figure S13. Thermogravimetric analysis of activated **TA**.

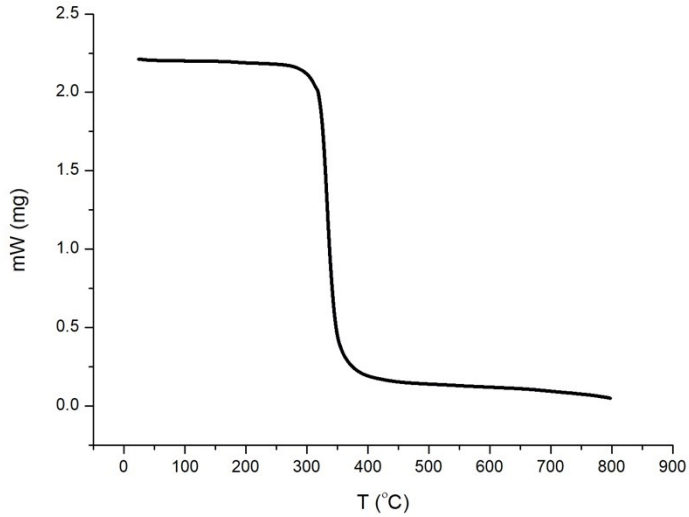

Figure S14. Thermogravimetric analysis of activated **MTA**.

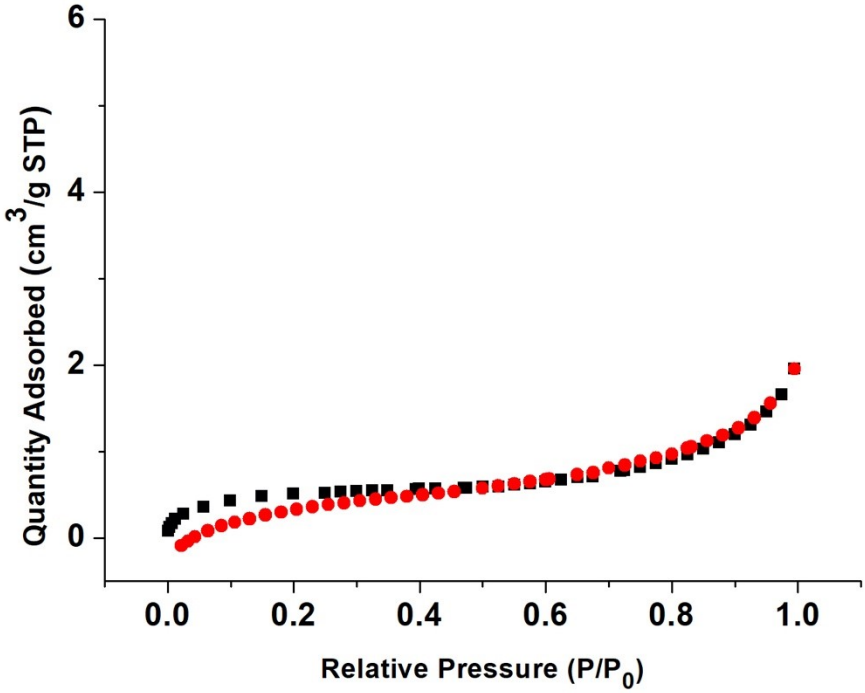

Figure S15. N_2 adsorption isotherm for activated **TI**. The BET surface area value is 1.67 m^2/g. Adsorption, black symbols; desorption, red symbols.

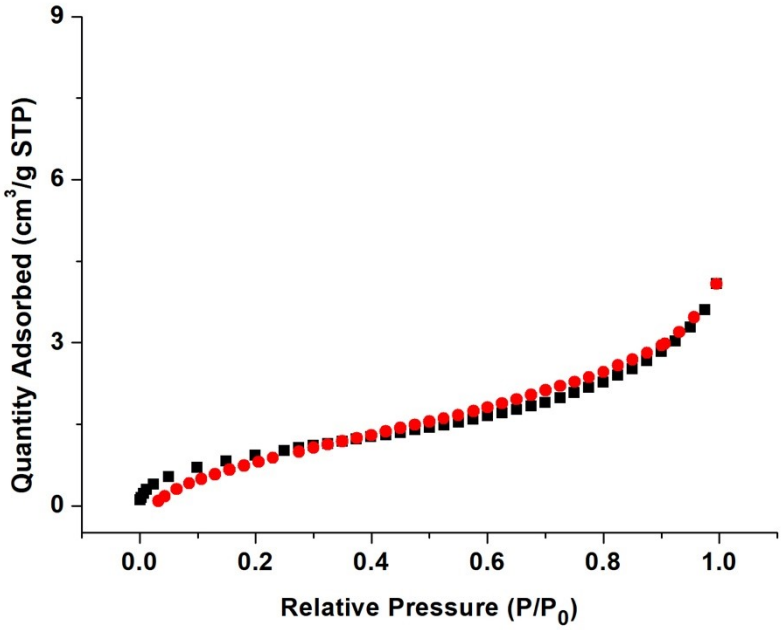

Figure S16. N_2 adsorption isotherm for activated **TA**. The BET surface area value is 3.65 m^2/g. Adsorption, black symbols; desorption, red symbols.

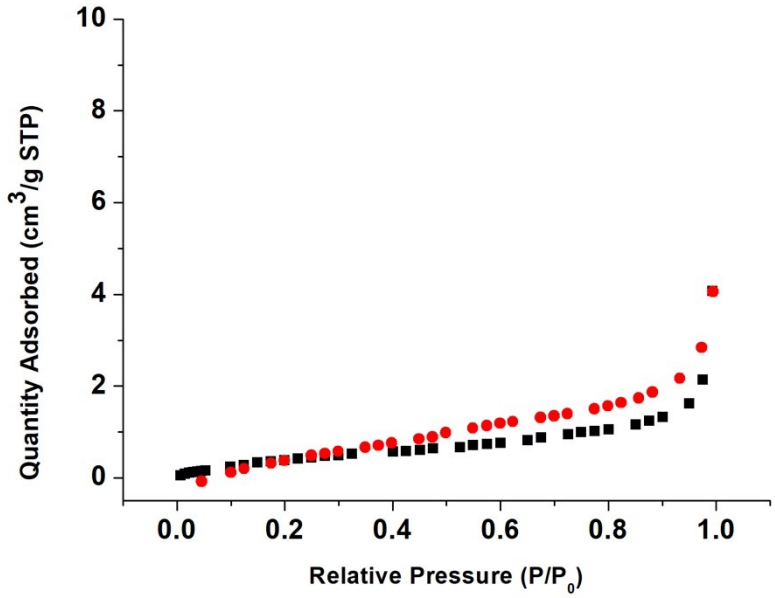

Figure S17. N_2 adsorption isotherm for activated **MTA**. The BET surface area value is 1.74 m^2/g. Adsorption, black symbols; desorption, red symbols.

Vapor-phase adsorption measurements

For each single-component **1-CBU** or **2-CBU** adsorption experiment, an open 5 mL vial containing 0.020 g of activated guest-free **TI/TA/MTA** adsorbent was placed in a sealed 20 mL vial containing 2 mL of **1-CBU** or **2-CBU**. Before measurements, the crystals were heated at 30 °C for 30 minutes to remove the surface-physically adsorbed vapor. Uptake in the **1-CBU** or **2-CBU** crystals was measured by completely dissolving the crystals in $CDCl_3$ by ^1H NMR.

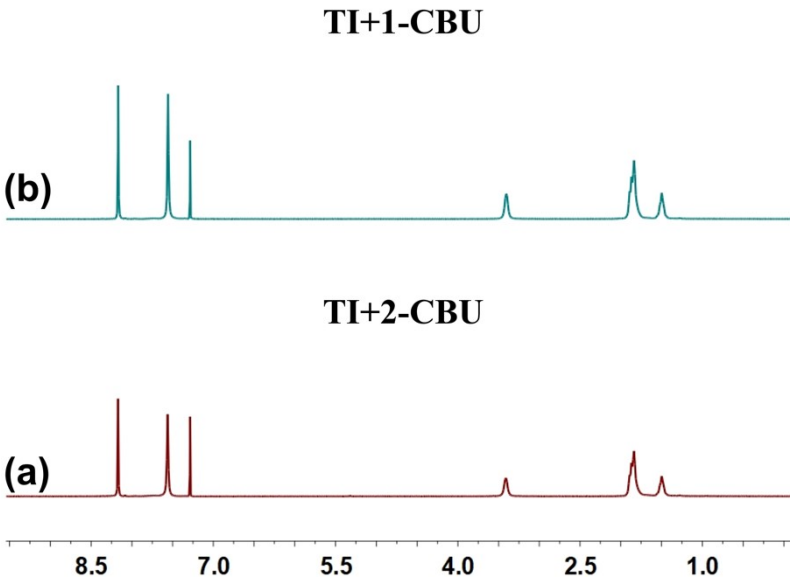

Figure S18. ^{1}H NMR spectra (400 MHz, $CDCl_3$, 293 K) of activated **TI** after exposure to (a) **2-CBU** vapor and (b) **1-CBU** vapor. The results indicated that there is no absorption of the chorobutane isomers.

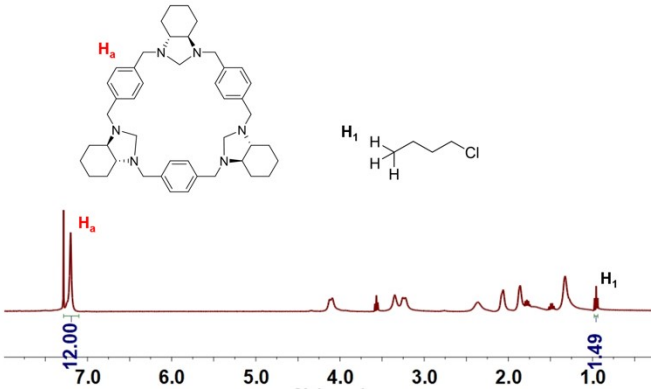

Figure S19. ^{1}H NMR spectrum (400 MHz, $CDCl_3$, 293 K) of activated **TA** after adsorption of **1-CBU** vapor. The integration can be calculated as about 0.5 equiv. of **1-CBU** per **TA** molecule.

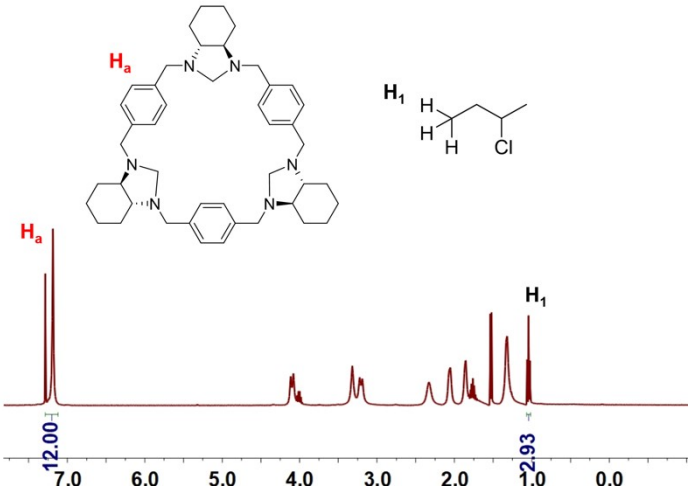

Figure S20. ^{1}H NMR spectrum (400 MHz, $CDCl_3$, 293 K) of activated **TA** after adsorption of **2-CBU** vapor. The integration can be calculated as about 1 equiv. of **2-CBU** per **TA** molecule.

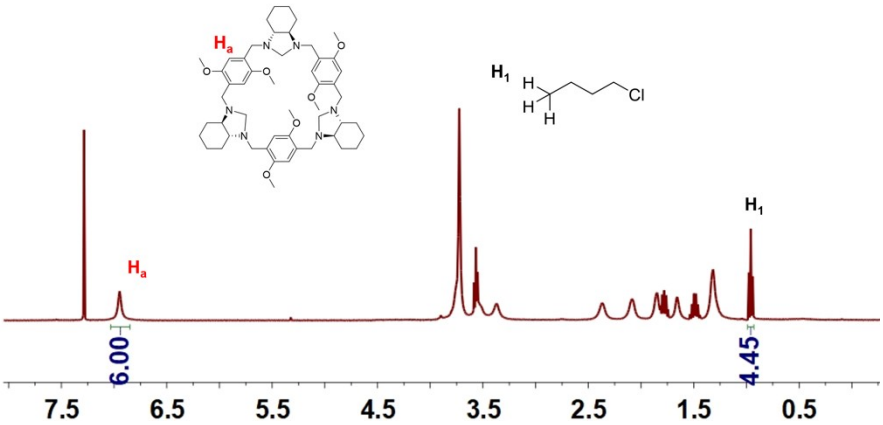

Figure S21. ^{1}H NMR spectrum (400 MHz, $CDCl_3$, 293 K) of activated **MTA** after adsorption of **1-CBU** vapor. The integration can be calculated as about 1.5 equiv. of **1-CBU** per **MTA** molecule.

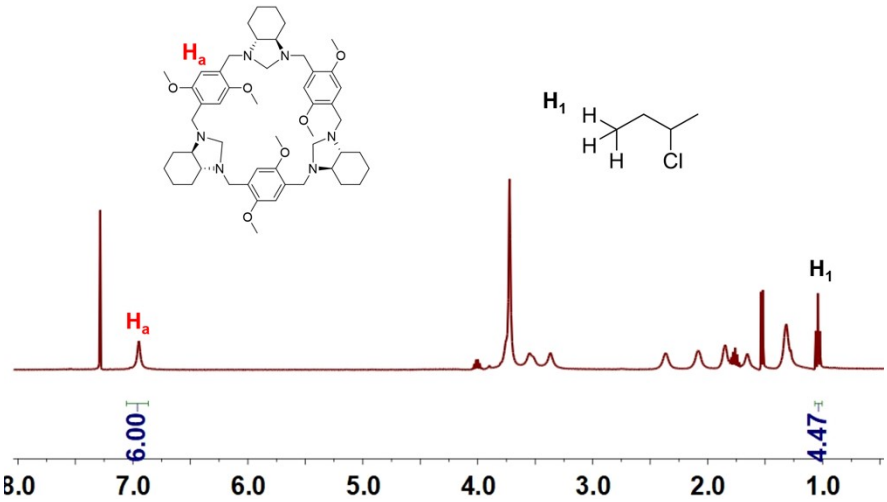

Figure S22. ^{1}H NMR spectrum (400 MHz, $CDCl_3$, 293 K) of activated **MTA** after adsorption of **2-CBU** vapor. The integration can be calculated as about 1.5 equiv. of **2-CBU** per **MTA** molecule.

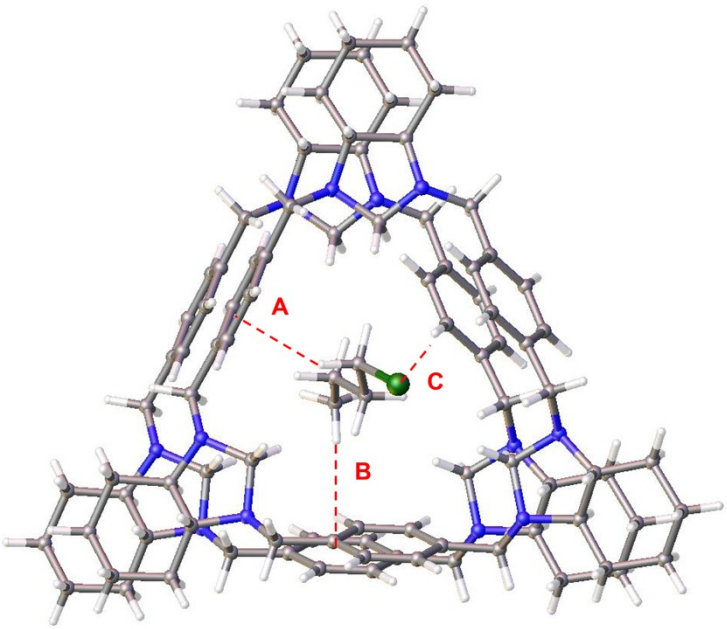

Figure 23. The crystal structure of **2TA⊃1-CBU**. C−H···Cl interaction parameters are as follows. H···Cl distance (Angstroms), C−H···Cl angle (degrees): C, 2.96, 167.2; H···π plane distance (Angstroms): A, 2.70; B, 2.99.

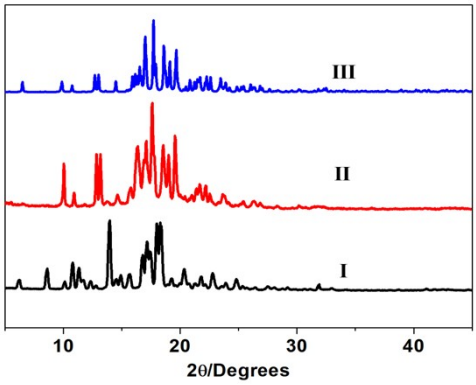

Figure S24. Powder X-ray diffraction patterns: (I) activated **TA**; (II) activated **TA** after adsorption of **1-CBU**; (III) simulated from single crystal structure of **2TA⊃1-CBU**.

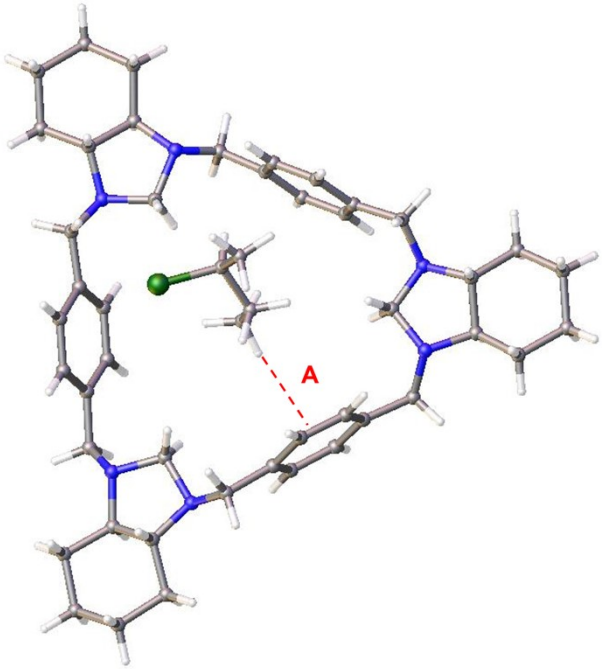

Figure 25. The crystal structure of **TA⊃2-CBU**. H···π plane distance (Angstroms): A, 2.96.

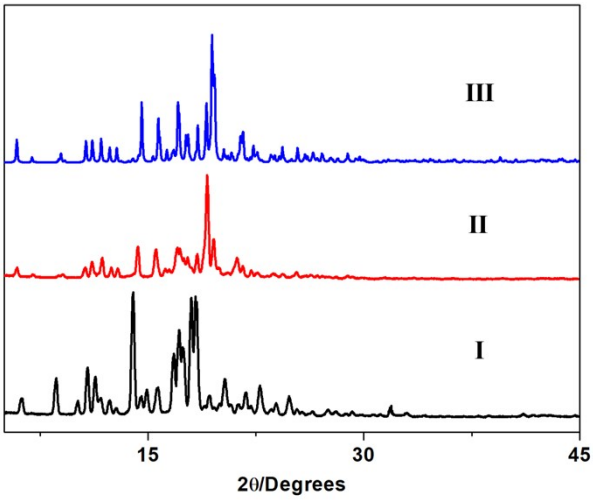

Figure S26. Powder X-ray diffraction patterns: (I) activated **TA**; (II) activated **TA** after adsorption of **2-CBU**; (III) simulated from single crystal structure of **TA⊃2-CBU**.

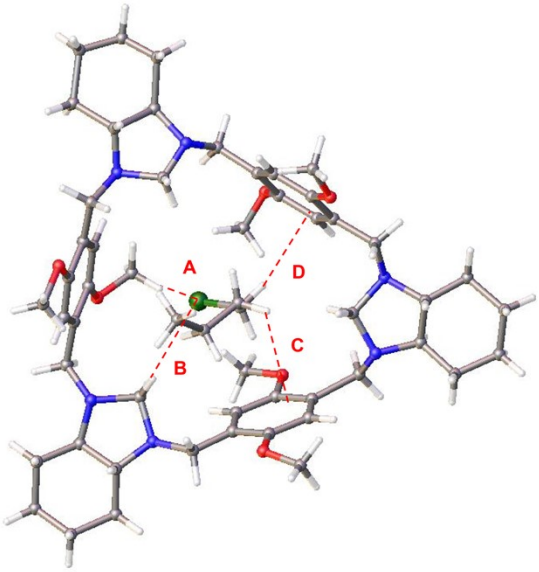

Figure 27. The crystal structure of **MTA@1-CBU**. C−H···Cl interaction parameters are as follows. H···Cl distance (Angstroms), C−H···Cl angle (degrees): A, 2.90, 123.6; B, 2.82, 124.4. H···π plane distance (Angstroms): C, 2.73; D, 2.88.

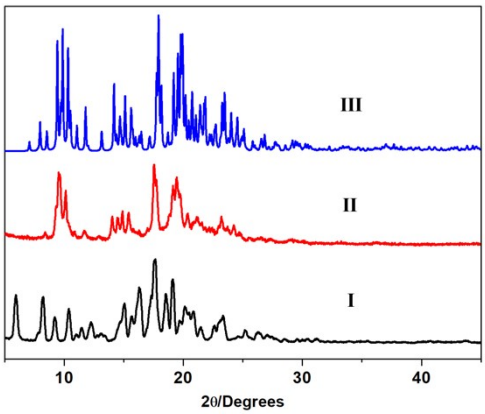

Figure S28. Powder X-ray diffraction patterns: (I) activated **MTA**; (II) activated **MTA** after adsorption of **1-CBU**; (III) simulated from single crystal structure of **MTA@1-CBU**.

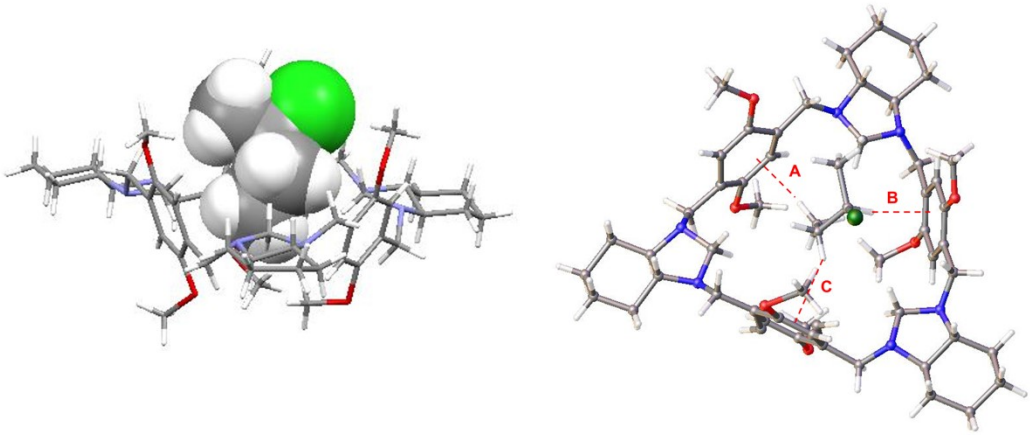

Figure S29. The crystal structure of **MTA@2-CBU**. C−H···π interaction parameters are as follows. H···π plane distance (Angstroms): A, 2.68; B, 3.01; C, 2.84.

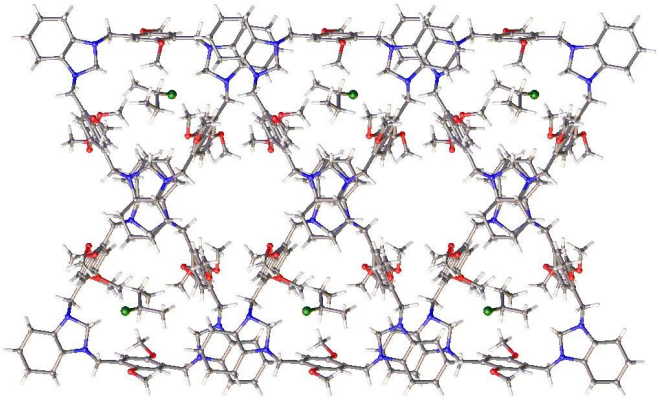

Figure S30. The packing structure of **MTA@2-CBU**. The crystal structure of **MTA@2-CBU** was very similar to that of **MTA@1-CBU**. In the crystal structure of **MTA@2-CBU**, **2-CBU** in the extrinsic channel is extremely disordered which can hardly be refined.

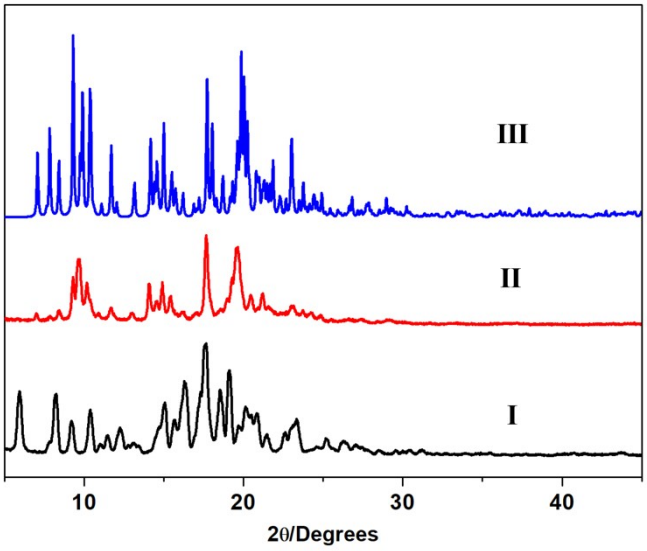

Figure S31. Powder X-ray diffraction patterns: (I) activated **MTA**; (II) activated **MTA** after adsorption of **2-CBU**; (III) simulated from single crystal structure of **MTA@2-CBU**.

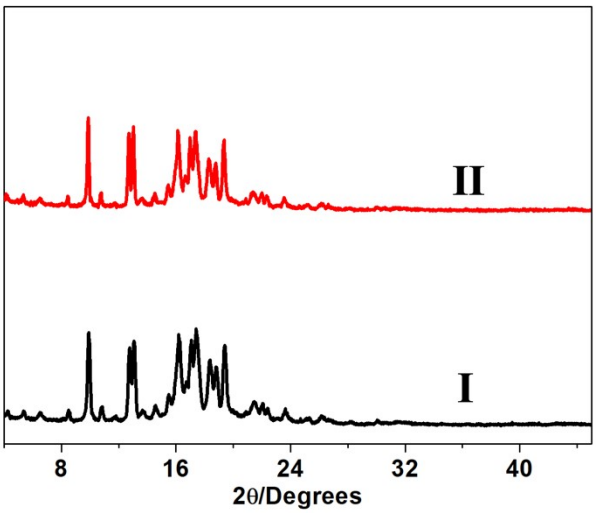

Figure S32. Powder X-ray diffraction patterns: (I) activated **TA** after adsorption of **1-CBU**; (II) **1-CBU**-loaded **TA** after exposure to **2-CBU** vapor. The PXRD patterns of **1-CBU**-loaded **TA** before and after exposure to **2-CBU** vapors were almost same, indicating that the crystal to crystal phase transformation from **TA⊃2-CBU** into **2TA⊃1-CBU** didn't happen.

Selective adsorption experiments of activated MTA/TA toward 1-CBU/2-CBU mixture

For the selective adsorption experiments, an open 5 mL vial containing 0.020 g of activated guest-free **TA/MTA** was placed in a sealed 20 mL vial containing 2 mL of the **1-CBU** and **2-CBU** mixture (*v*:*v* = 1:1). Before measurements, the crystals were heated at 30 °C for 30 minutes to remove the surface physically adsorbed vapor. Uptake in the **1-CBU** or **2-CBU** crystals was measured by completely dissolving the crystals in $CDCl_3$ by ^1H NMR. For cycling performance investigation, **1-CBU**-loaded **TA** powders were heated under vacuum at 120 °C overnight to release **1-CBU** from **TA.**

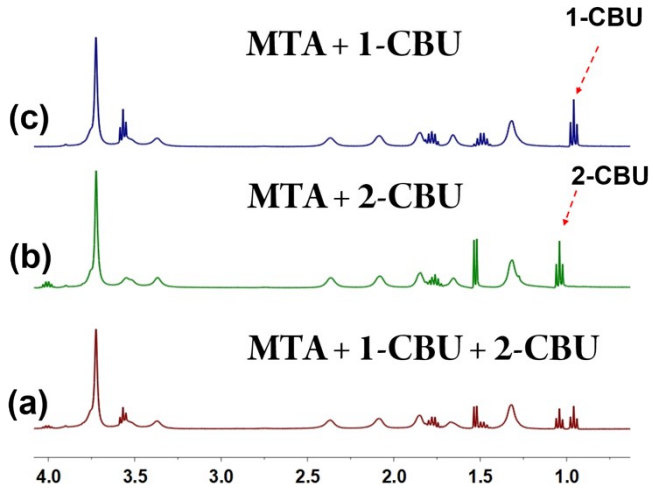

Figure S33. Magnified ^{1}H NMR spectra of activated **MTA** after adsorption of (a)**1-CBU/2-CBU** mixture, (b) **2-CBU** (pure) and (c) **1-CBU** (pure).

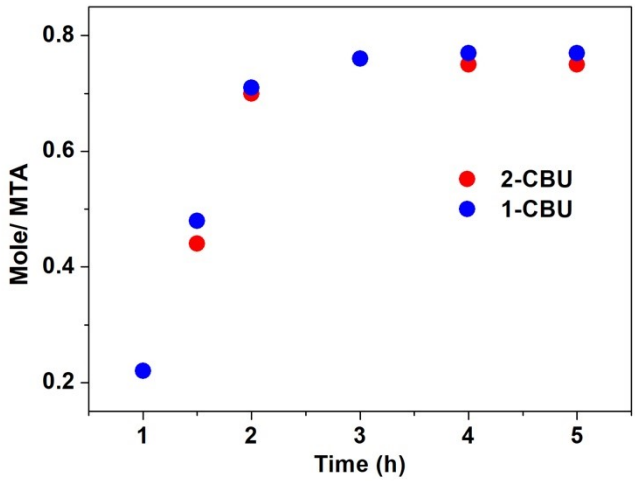

Figure S34. Time-dependent solid−vapor sorption plot of activated **MTA** for **1-CBU/2-CBU** mixture vapor.

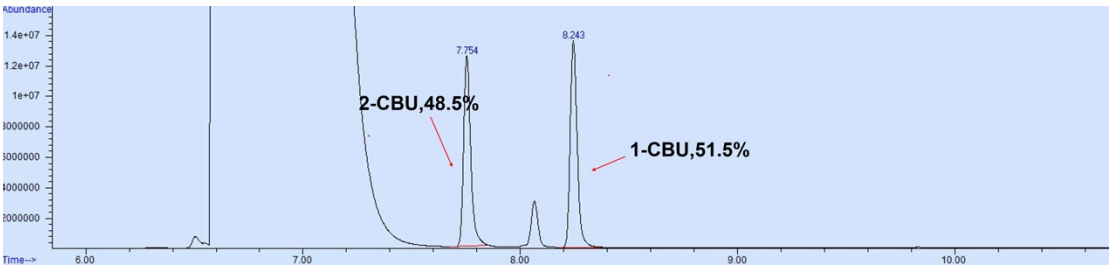

Figure S35. Relative **1-CBU/2-CBU** uptake in crystalline **MTA** measured by gas chromatography.

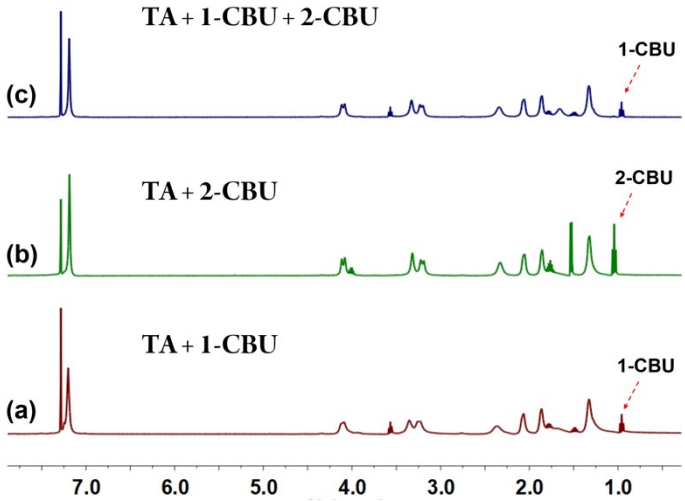

Figure S36. Magnified ^{1}H NMR spectra of activated **TA** after adsorption of (a) **1-CBU** (pure), (b) **2-CBU** (pure) and (c) **1-CBU**/**2-CBU** mixture.

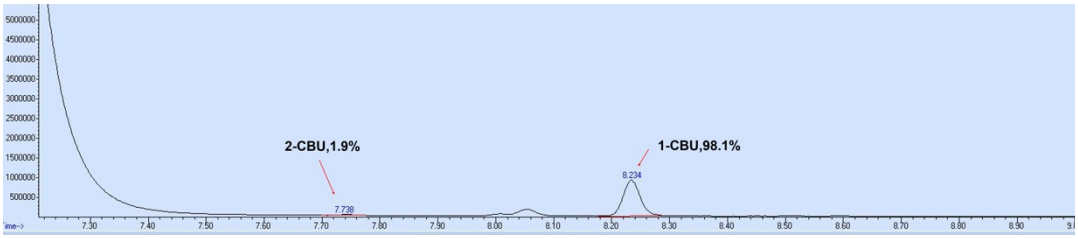

Figure S37. Relative **1-CBU**/**2-CBU** uptake in crystalline **TA** measured by gas chromatography.

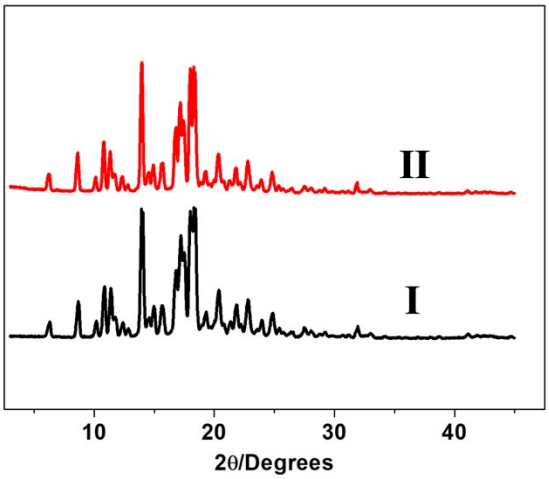

Figure S38. PXRD spectra of (I) activated **TA** and (II) activated **TA** immersed in water for 7 days.

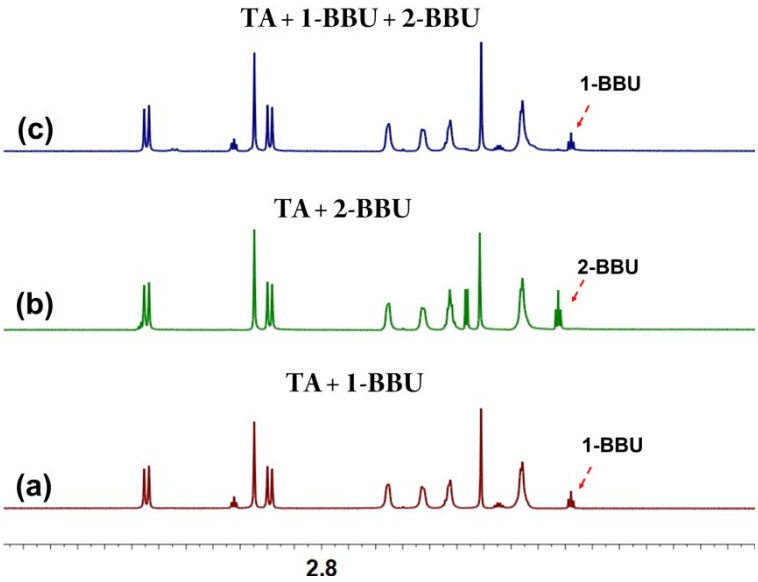

Figure S39. Partial ^{1}H NMR spectra of activated **TA** after adsorption of (a) **1-BBU** (pure), (b) **2-BBU** (pure) and (c) **1-BBU/2-BBU** mixture.

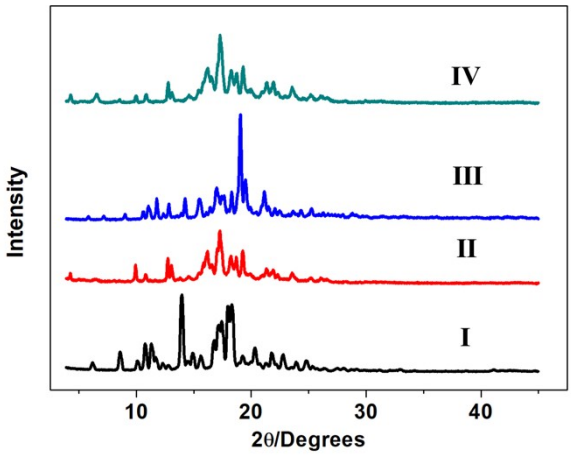

Figure S40. PXRD patterns of: (I) activated **TA**; (II) activated **TA** after exposure to 1-bromobutane (**1-BBU**) vapor; (III) activated **TA** after exposure to 2-bromobutane (**2-BBU**) vapor; (IV) activated **TA** after exposure to the mixture vapor of **1-BBU** and **2-BBU (1:1)**.

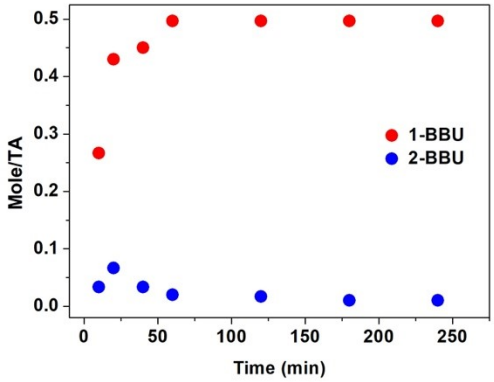

Figure S41. Time-dependent solid−vapor sorption plot of activated **TA** for **1-BBU**/**2-BBU** mixture vapor.

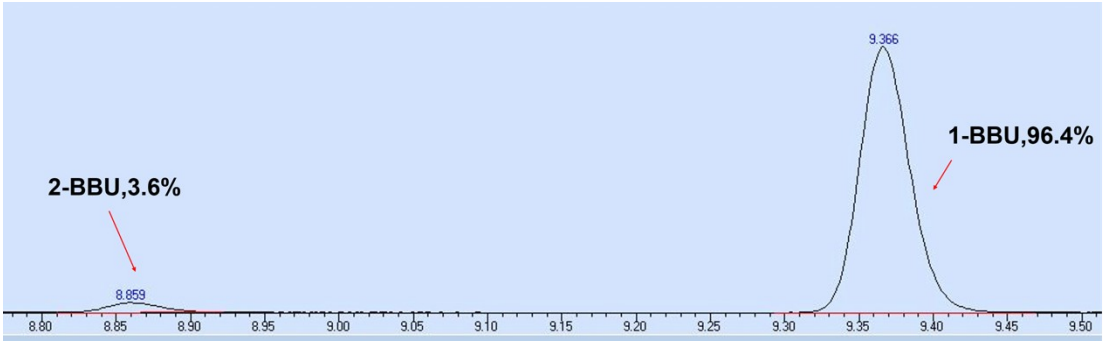

Figure S42. Relative **1-BBU**/**2-BBU** uptake in crystalline **TA** measured by gas chromatography.

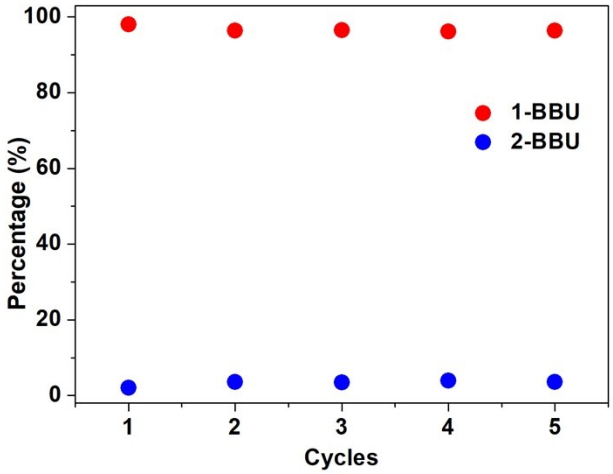

Figure S43. Relative uptake of **1-BBU** and **2-BBU** for five cycles.

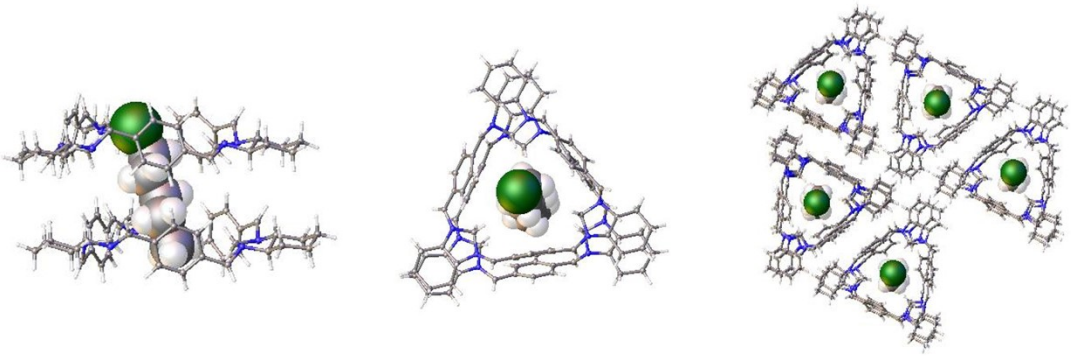

Figure S44. Ball-stick views of the crystal structure of **2TA⊃1-CP**.

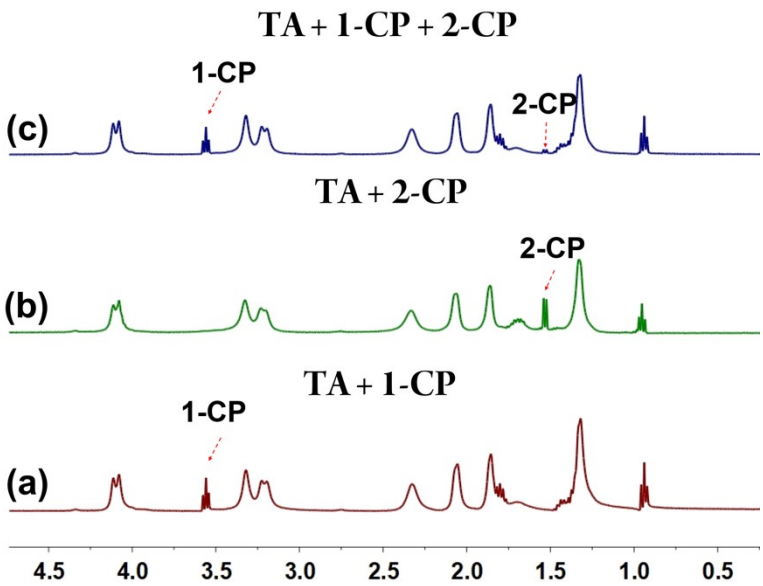

Figure S45. Partial ^{1}H NMR spectra of activated **TA** after adsorption of (a) **1-CP** (pure), (b) **2-CP** (pure) and (c) **1-CP/2-CP** mixture.

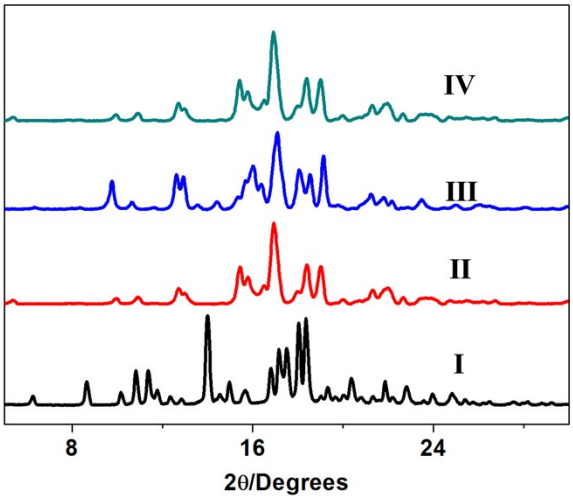

Figure S46. PXRD patterns of: (I) activated **TA**; (II) activated **TA** after exposure to 1-chloropentane (**1-CP**) vapor; (III) activated **TA** after exposure to 2-chloropentane (**2-CP**) vapor; (IV) activated **TA** after exposure to the mixture vapor of **1-CP** and **2-CP** **(1:1)**.

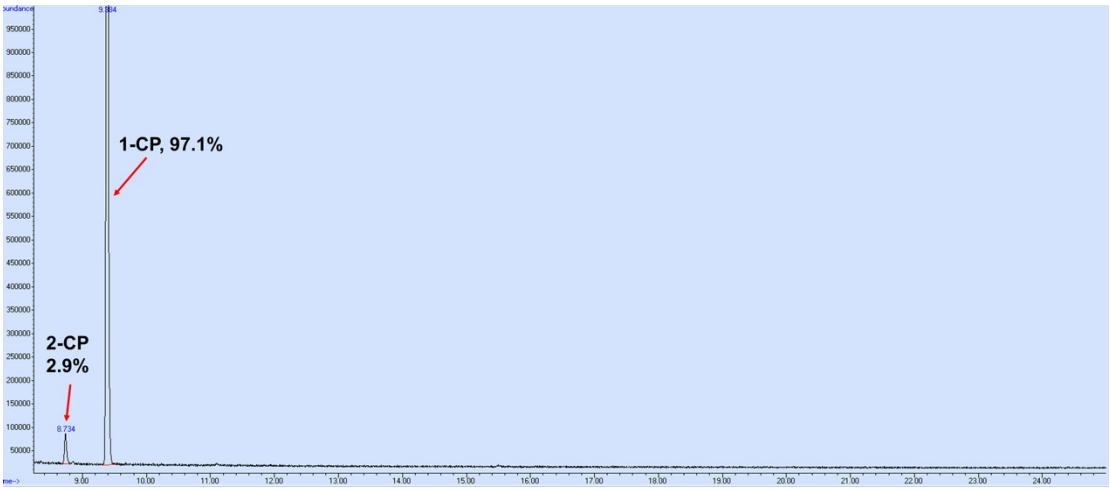

Figure S47. Relative **1-CP**/**2-CP** uptake in crystalline **TA** measured by gas chromatography.

X-ray crystal data

	2TA⊃1-CBU	**TA⊃2-CBU**	**2TA⊃1-CP**
Collection Temperature	120 K	120 K	120K
Sum Formula	$C_{47}H_{64.5}Cl_{0.5}N_6$	$C_{49}H_{69}ClN_6$	$C_{95}H_{119}ClN_{12}$
Mr	731.27	777.55	1464.46
Crystal System	orthorhombic	triclinic	monoclinic
Space Group	$P2_12_12$	P1	C2
a [Å]	17.8982(5)	10.9057(15)	34.933(2)
b [Å]	41.8156(12)	14.2504(17)	11.7740(6)
c [Å]	5.6166(2)	16.844(2)	22.6543(13)
α [°]	90	107.383(7)	90
β [°]	90	104.681(8)	114.401(3)
γ [°]	90	104.350(7)	90
V [Å3]	4203.6(2)	2263.4(5)	8485.4(8)
Z	4	2	4
D*calcd* [g cm-3]	1.155	1.141	1.146
μ[mm-1]	0.802	0.124	0.098
F(000)	1588.0	844.0	3160.0
2*θ* range [°]	5.37–133.158	4.122–52.742	4.426–56.822
Reflections collected	21071	82923	85840
Independent reflections, *Rint*	7304, 0.0338	18192, 0.0271	20836,0.1378
Data /restraints /parameters	7304/1100/764	18192/618/1157	20836/1/975
Final *R*1 values ($I > 2\sigma(I)$)	0.0616	0.0496	0.0865
Final *R*1 values (all data)	0.0678	0.0528	0.1702
Final $wR(F_2)$ values (all data)	0.1612	0.1423	0.2764
Goodness-of-fit on F^2	1.091	1.028	1.017
Largest difference peak and hole [e.A-3]	0.18/-0.26	0.75/-0.42	1.23/-0.61
CCDC	2056801	2056802	2079899

	MTA@1-CBU	**MTA@2-CBU**
Collection Temperature	120.04 K	120.0 K
Mr	3920.30	957.70
Crystal System	Monoclinic	Monoclinic
Space Group	$P2_1$	$P2_1$
a [Å]	9.9529(3)	9.8761(2)
b [Å]	49.9513(16)	49.9783(10)
c [Å]	12.3951(3)	12.5730(3)
α [°]	90	90

β [°]	113.5250(10)	113.0610(10)
γ [°]	90	90
V [Å3]	5650.2(3)	5710.0(2)
Z	1	4
D*calcd* [g cm-3]	1.152	1.114
μ[mm-1]	0.131	0.998
F(000)	2119.0	2072.0
2θ range [°]	4.464 – 49.992	7.074– 136.612
Reflections collected	44278	44398
Independent reflections, *Rint*	18680, 0.0605	18565, 0.0324
Data /restraints /parameters	18680/2030/2040	18565/1698/1643
Final $R1$ values ($I > 2\sigma(I)$)	0.0944	0.0814
Final $R1$ values (all data)	0.1260	0.0866
Final $wR(F_2)$ values (all data)	0.2798	0.2251
Goodness-of-fit on F^2	1.051	1.018
Largest difference peak and hole [e.A-3]	1.02/-0.42	0.58/-0.723
CCDC	2056799	2056800

Crystallization methods: 5 mg of dry **TA** or **MTA** powders were put in small vials where 2 mL of **1-CBU**, **1-CP** or **2-CBU** were added, respectively. The resultant transparent solutions were allowed to evaporate slowly to give colorless crystals in 2 to 3 days.

References

S1. N. Kuhnert, C. Straßnig, and M.Lopez-Periago, *Tetrahedron: Asymmetry* 2002, **13**, 123–128.

S2. J. Gawronski, K. Gawronska, J. Grajewski, M. Kwit, A. Plutecka and U. Rychlewska *Chem. Eur. J.* 2006, **12**, 1807–1817.

S3. M. Chadim, M. Budesinsky, J. Hodacova, J. Zavada and P. C. Junk, *Tetrahedron: Asymmetry* 2001, **12**, 127–133.

S4. Y. Zhou, K. Jie, R. Zhao, E. Li and F. Huang, *J. Am. Chem. Soc.* 2020, **142**, 6957–6961.